

## **DIRECT NUMERICAL SIMULATION (DNS) OF FULLY DEVELOPED TURBULENT CHANNEL FLOW WITH HEAT TRANSFER FOR MODERATELY HIGH REYNOLDS NUMBERS**

**Hugo D. Pasinato**

*Dpto. Ing. Electromecánica, FRP-Universidad Tecnológica Nacional, Avda. Almaguero 1033,  
3100 Paraná, Argentina; hpasinato@frp.utn.edu.ar; Tel. +54-343-424 3054; Fax. +54-343-424 3054*

**Keywords:** Turbulent heat transfer, velocity-temperature dissimilarity, DNS.

**Abstract.** Direct Numerical Simulation (DNS) is a very powerful tool to investigate turbulent flow; e.g. to scrutinize fundamental physical aspects, to validate turbulent models, etc. In the past, however, DNS had the limitation of low-Reynolds number effects, since almost all these simulations were done for relatively low Reynolds numbers. Owing to the rapid increase in the computer power, moderately high Reynolds number turbulent flows are now been investigated using DNS. In the present study, DNS of fully developed turbulent channel flow with heat transfer, at four Reynolds numbers based on friction velocity and channel half width ( $Re_\tau = \delta u_\tau / \nu$ ) up to  $Re_\tau = 930$  and at molecular Prandtl number equal to 1 are reported. The objective of this study is to analyze the Reynolds number dependency of the flow and heat transfer turbulent quantities. The computed fields are also examined to investigate some aspects related with the similarity/dissimilarity of the fluctuations of the temperature and the streamwise velocity.

## 1 INTRODUCTION

Wall bounded turbulent flows with heat transfer impact a large number of technologically important applications. For this reason this topic has received continuous attention in the last decades. In such flows there are many physical aspects related with momentum and heat transfer, that deserve to be studied in detail aiming at to improve the prediction of the transfer coefficients at the wall, to study the momentum and heat similarity/dissimilarity in the wall layer, to improve turbulence models, etc. The study of the physical phenomena of a turbulent flow near a solid boundary, however, have always been a major challenge, not only for those using numerical techniques, but also for experimentalists. For numerical simulations the major obstacles were, and continue to be, to accurately resolve the smallest and fastest scales near the wall, the need for high performance computers to simulate flows with high Reynolds numbers, etc. Experimentalists, on the other hand, have among other the challenges of measure without disrupting the flow, to maintain a small measurement volume to avoid spatially averaging the smallest scales when the size of the experimental facilities are important, and give special attention to the calibration and response of the instrumentation.

In the last decades there was an enormous research effort on wall bounded turbulence in pipes, channels and boundary layers at high Reynolds numbers, as new experimental facilities and advance in experimental diagnostics (Marusic et al., 2010), as well as new big computer clusters have been incorporated; e.g. notably the super cluster Blue Gene Sequoia, at the Lawrence Livermore National Laboratory. All these new efforts have brought a critical review of almost all aspects of wall bounded turbulent flows in pipes, channels and boundary layers, since the mean velocity profile near the wall, the von Karman 'constant' value, and the friction velocity and kinematic viscosity as the parameters to construct the universal scaling next to the wall, among other aspects.

Since channel flow is one of the simplest geometry that allows isolating complex physical phenomena, at the beginning channel geometry was one of the most used. At this time only channel flows with very low Reynolds numbers equal to 150 or 180 ( $Re_\tau = u_\tau \delta / \nu$ , where  $u_\tau$  is the friction velocity,  $\delta$  is half the distance between walls and  $\nu$  is the kinematic viscosity) were simulated (Kim et al., 1987; Moser et al., 1999). But in recent years DNS with more and more higher Reynolds numbers are being simulated (Hoyas and Jimenez, 2008; Kozuka et al., 2008) (it is appropriate to say that nowadays there is a renewed effort for DNS in pipes for high Reynolds numbers, since pipe flow experimental facilities seems to be less expensive than those for channel flows).

In this study the results of DNS at four Reynolds numbers up to 930, for a channel flow with heat transfer is presented. These simulations are the first step to do DNS of perturbed turbulent flows with heat transfer for moderately high Reynolds numbers. Therefore, the goal of this paper is to do a comparison of the computed statistics with similar results from the literature, discussing aspects related with the scaling and the Reynolds number dependence of the data, as well as to discuss a few aspects of the velocity-temperature similarity/dissimilarity for fully developed flows for this range of Reynolds numbers.

## 2 NUMERICAL DETAILS

In this section the computational domain sizes, the grids, and other numerical details for the four DNS cases are presented.

In this paper,  $\hat{u}$ ,  $\hat{v}$ , and  $\hat{w}$  are the instantaneous velocities in the stream-wise ( $x$ ), wall-normal ( $y$ ), and span-wise ( $z$ ) directions, respectively. All instantaneous variables are decomposed as

Table 1: Simulation parameters for the four direct numerical simulations of a channel flow with heat transfer.

<i>Case</i>									$\Delta_y^+$
<i>name</i>	<i>Line</i>	$Re_\tau$	$Re_{2\delta}$	$Lx$	$Lz$	$Nx \times Ny \times Nz$	$\Delta_x^+$	$\Delta_z^+$	<i>max.</i>
<i>Re150</i>	solid	149	4289	$5\pi$	$3/2\pi$	$256 \times 144 \times 128$	9.20	4.90	5.28
<i>Re300</i>	— —	302	9379	$3\pi$	$4/3\pi$	$256 \times 240 \times 256$	11.0	4.90	6.59
<i>Re600</i>	—.—	602	20592	$2.25\pi$	$\pi$	$512 \times 336 \times 256$	8.28	7.36	9.90
<i>Re930</i>	.....	902	32489	$2.25\pi$	$\pi$	$1024 \times 464 \times 512$	6.40	5.70	10.50

mean values and fluctuations; e.g.,  $\hat{u} = U + u$ . The brackets  $\langle \cdot \rangle$  represent averaging over homogeneous directions, usually over wall-parallel planes and times.

The nondimensionalization of the variables in this study is done using the friction velocity  $u_\tau$ , the viscous length scale  $\nu/u_\tau$ , and the friction temperature  $T_\tau = q_w/\rho c_p u_\tau$ . Here,  $\theta$  is the dimensionless temperature,  $q_w$  is the heat flux at the wall, and  $c_p$  and  $\rho$  are the constant pressure-specific heat coefficient and density, respectively.

The numerical method, the geometry, the initial and boundary condition and other numerical aspects for velocity and temperature is as in the channel flow reported in [Pasinato \(2007, 2011\)](#). The Prandtl number of the fluid is equal to 1. Buoyancy effects are neglected, as the temperature is considered as a passive scalar. For the thermal field (the boundary conditions for temperature) a uniform heat source is used, similar to Case I solved in [Kim and Moin \(1989\)](#), in which a dimensionless source term equal to  $2/(Re_\tau Pr)$  was used. In the present study, however, the source is a constant energy source uniformly distributed in the domain, equal to  $q_w/\delta$  in the dimensional form and in the dimensionless form equal to 1. For this case, the dimensionless temperature  $\theta = (T_w - T)/T_\tau$  is zero at the walls, and the Reynolds-averaged problem for the longitudinal velocity and temperatures in dimensionless form are analogous, since their mean differential equations and mean boundary conditions are similar.

Table 1 show the Case name, the line type used in the plots for the present results, the nominal friction Reynolds number  $Re_\tau = u_\tau \delta/\nu$ , the Reynolds numbers as a function of the mean velocity and twice the separation between plates  $Re_{2\delta} = U2\delta/\nu$ , the size of the computational domain, and the grid spacing for every DNS data of a channel flow with heat transfer reported here.

As regarding the computational domain size, it is appropriate to comment that in the last decade the measurements of the spectra have revealed the presence of very large scales motion, that contribute significantly to the total energy content at all positions away from the wall, for high Reynolds turbulent bounded flows ([Hites, 1997](#); [Jimenez, 1998](#); [Kim and Adrian, 1999](#)). The characteristic scale of these structures is of  $10\delta$  in channels ( $10R$  in pipes, where  $R$  is the pipe radius). This finding has motivated that new direct numerical simulations with very large computational domains were used for high Reynolds numbers, in order to study the importance of these structures. Although, as commented above, their energy contribution is mainly away from the wall and more important for high Reynolds numbers, it has raised new criteria to define the size of the computational domain in numerical simulations. In the present simulations, however, the computational domain has been defined as in [Moser et al. \(1999\)](#)'s DNS, looking at the inner region near the wall.

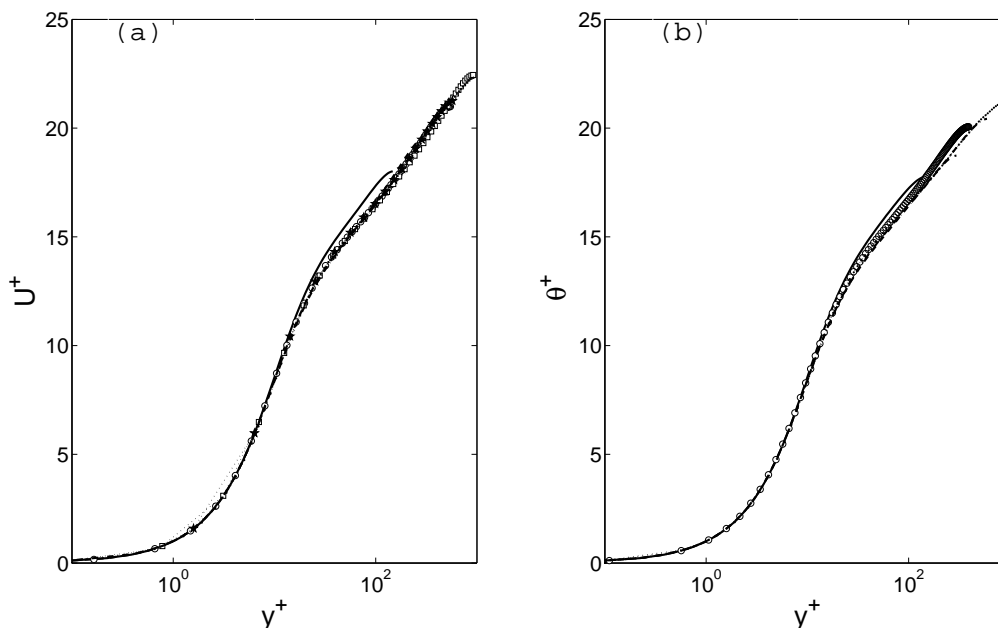


Figure 1: Longitudinal velocity and temperature mean values. Present results as in Table 1. (a) Mean velocity,  $U^+$ ;  $\star \cdot \star \cdot \star$ , Moser et al. (1999),  $Re_\tau = 590$ ;  $\circ \cdot \circ \cdot \circ$ , and  $\square \cdot \square \cdot \square$ , Jimenez and Hoyas (2008),  $Re_\tau = 550$  and 930, respectively. (b) mean temperature,  $\Theta^+$ ,  $\circ \cdot \circ \cdot \circ$ , Kozuka et al. (2008),  $Re_\tau = 395$ .

### 3 RESULTS AND DISCUSSION

Based on the classical theory of bounded turbulent flow, it is thought that for very high Reynolds numbers there exist a fully developed state of turbulence. If a proper scaling is used, it is thought that such kind of state of turbulence should present a universal behavior. This has been, for example, the spirit of the *law of the wall*, first proposed by von Karman in 1930 for the wall layer. This law is the result of the existence of an overlap layer between the inner region near the wall and the outer region afar from it, where the unique velocity scale is the friction velocity,  $u_\tau$ . One fundamental condition for the existence of this overlap layer next to a wall is that there exist a region far from the wall for viscosity to be important, but close enough to it for the total tangential stress not to be very different from its value  $u_\tau^2$  at the wall (Millikan, 1993; Tennekes and Lumley, 1972; Townsend, 1976). At the near-wall region the velocity and length scales are  $u_\tau$  and  $\nu/u_\tau$ , respectively. At the outer region these scales are the friction velocity and the length scale is  $\delta$ , half the distance between walls for a channel or a fraction of it. At the overlap layer the velocity and length scales are the friction velocity and the wall distance (as it restricts the size of the turbulence structures). Therefore  $u_\tau$  is the only velocity scale in the whole flow and is the link between the inner and the outer region.

As a result of this wall-scaling, a universal behavior is expected basically of the dimensionless mean value of the mean streamwise velocity, as it is specified by the *law of the wall*, which states that  $U^+ = \ln(y^+)/0.41 + 5.5$ , where 0.41 is the von Karaman 'constant' and the second number depend on the wall roughness and the Reynolds number (here 'constant' means that nowadays there is not a complete agreement whether it is a constant or actually a weak Reynolds number function). Here the old values published by Dean (1978) for channel flows are used, even though it is known that there are small differences in the value of  $\kappa$  for flows in

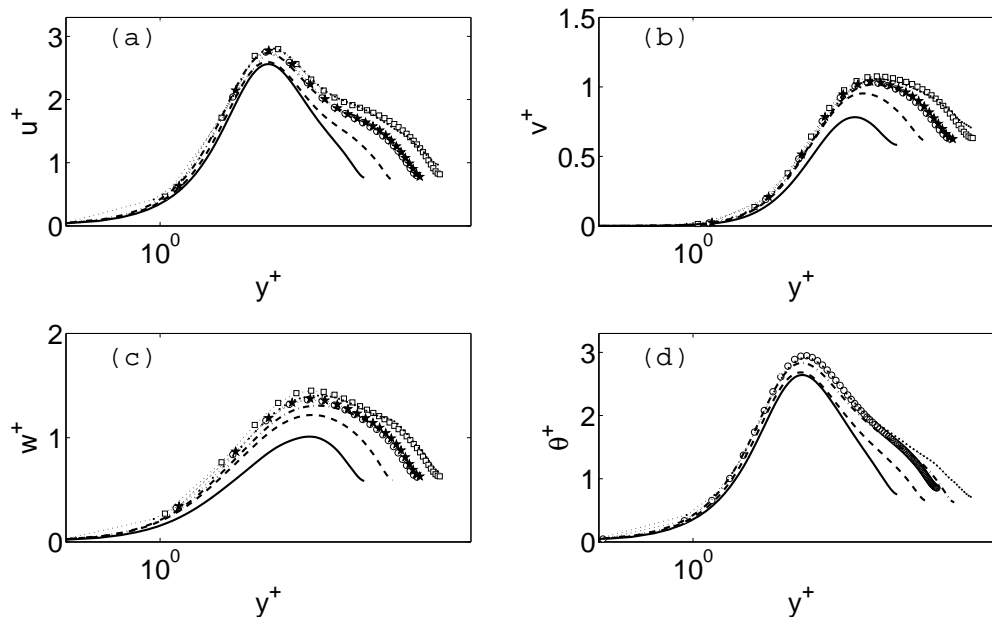


Figure 2: R.m.s. of fluctuation of velocity and temperature. Present results as in Table 1;  $\star \cdot \star \cdot \star$ , Moser et al. (1999),  $Re_\tau = 590$ ;  $\circ \cdot \circ \cdot \circ$ , and  $\square \cdot \square \cdot \square$ , Jimenez and Hoyas (2008),  $Re_\tau = 550$  and 930, respectively. (a)  $u^+$ ; (b)  $v^+$ ; (c)  $w^+$ ; (d)  $\theta^+$ .

pipes, channels and boundary layers.

Related with this physics of the developed state of turbulence, more universal behavior is expected in such overlap layer for other turbulent quantities when properly nondimensionalized (Townsend, 1976; Jimenez and Hoyas, 2008). In this trend a universal behavior is expected near the wall for the r.m.s. of the velocities fluctuation,  $u^+$ ,  $v^+$ ,  $w^+$ , the pressure fluctuation,  $p^+$ , the kinetic energy of the turbulence and its dissipation,  $\kappa^+$ , and  $\epsilon^+$ , respectively, among other. This universal behavior does not seem to be the case, however; in contrast, there exist a weak function of the Reynolds numbers of the major part of the turbulence quantities.

In the last decades several experimental and numerical studies have addressed this wall-scaling (Wei and Willmarth, 1989; Antonia and Kim, 1994; Kim et al., 1987; Moser et al., 1999; Jimenez and Hoyas, 2008; Hoyas and Jimenez, 2008), and the existence of a unique state of turbulence behavior for sufficiently large, but finite Reynolds number, is being questioned, and also has been questioned the logarithmic law for channels, pipes, and boundary layers, even though it seems to be the most likely behavior (Barenblatt, 1993; George et al., 2000). Also, the von Karman 'constant' seems to be not the same for channels, pipes or boundary layers flows, and the values for channels seem to be not the classical 0.41 and 5.5 values published by Dean (1978). On the other hand, the location of the maximal of the r.m.s of the velocity fluctuations seems to scale with the  $u_\tau$  and  $\nu/u_\tau$ , but their values are Reynolds dependent, and the same seems to be the case for the r.m.s of the pressure fluctuations and mean pressure.

In the following, a synthesis of the main results of the present numerical simulations for the four Reynolds numbers of the channel flow with heat transfer are presented, together with some discussion.

Figure 1-a shows the distribution of  $U^+$  with  $y^+$  for the 4 Reynolds together with the Moser et al. (1999)'s DNS data for  $Re_\tau = 590$  and the Jimenez and Hoyas (2008)'s DNS data for  $Re_\tau = 547$  and 934, and Figure 1-b shows the  $\Theta^+$  with  $y^+$  together with Kozuka et al. (2008)'s

DNS data for  $Re_\tau = 395$ . In Figure 2a-c the r.m.s of velocities and again the data from Moser's and Jimenez's group are included, and in Figure 2-d the r.m.s. of the temperature fluctuation is shown with the Kozuka et al. (2008)'s data for  $Re_\tau = 395$ . Note that in general there is a good agreement in the comparisons of these turbulent quantities.

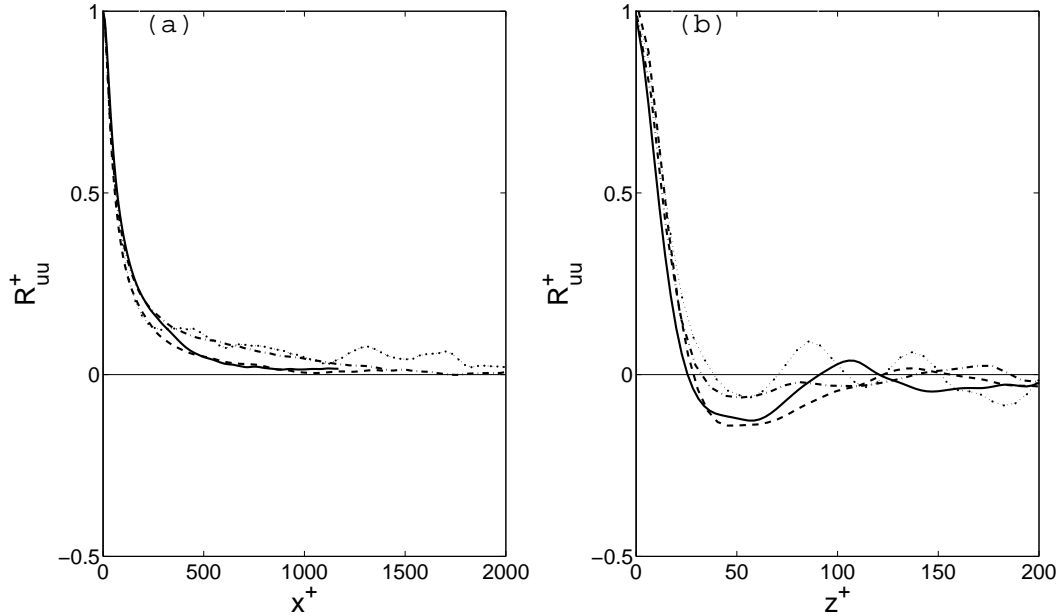


Figure 3: Two-point correlations for the longitudinal velocity fluctuation at  $y^+ \simeq 18$ . Lines as in Table 1. (a)Streamwise; (b)Spanwise.

Table 2: Wall values for different turbulent quantities; where  $\epsilon^+$  is the total turbulence dissipation,  $\epsilon_{11}^+$  and  $\epsilon_{33}^+$  are the longitudinal and spanwise turbulence dissipation,  $\epsilon_\theta^+$  is the turbulence dissipation of the thermal field,  $\omega_{11}^+$  and  $\omega_{33}^+$  are the longitudinal and spanwise vorticity components, and  $(p,x)^+$ ,  $(p,y)^+$  and  $(p,z)^+$  are the r.m.s. of the streamwise, wall-normal and spanwise gradient of the pressure fluctuation.

Case name	$\epsilon^+$	$\epsilon_{11}^+$	$\epsilon_{33}^+$	$\epsilon_\theta^+$	$\omega_{11}^+$	$\omega_{33}^+$	$p^+$	$(p,x)^+$	$(p,y)^+$	$(p,z)^+$
Re150	0.155	0.122	0.033	0.127	0.182	0.352	1.440	0.046	0.004	0.067
Re300	0.199	0.146	0.053	0.152	0.227	0.382	1.889	0.058	0.005	0.080
Re600	0.239	0.184	0.055	0.182	0.232	0.423	2.170	0.067	0.007	0.084
Re930	0.259	0.201	0.058	0.200	0.250	0.452	2.401	0.074	0.008	0.086

In Figures 3-a and 3-b the streamwise and spanwise two-point correlations for  $u$  are shown, respectively, for  $y^+ \simeq 18$ . Figure 3-a shows that the streamwise structures near the wall scales with the inner variables for the different Reynolds numbers, showing also (as it is known) that the length of the streamwise structures is approximately 1000 wall units. On the other hand, in Figure 3-b is seen (as it is also known) that the spanwise separation of these structures is approximately 100 wall units, for all Reynolds numbers. Therefore, the size and spanwise separation of the streamwise vortical near-wall structures seems to scale with the inner scales,

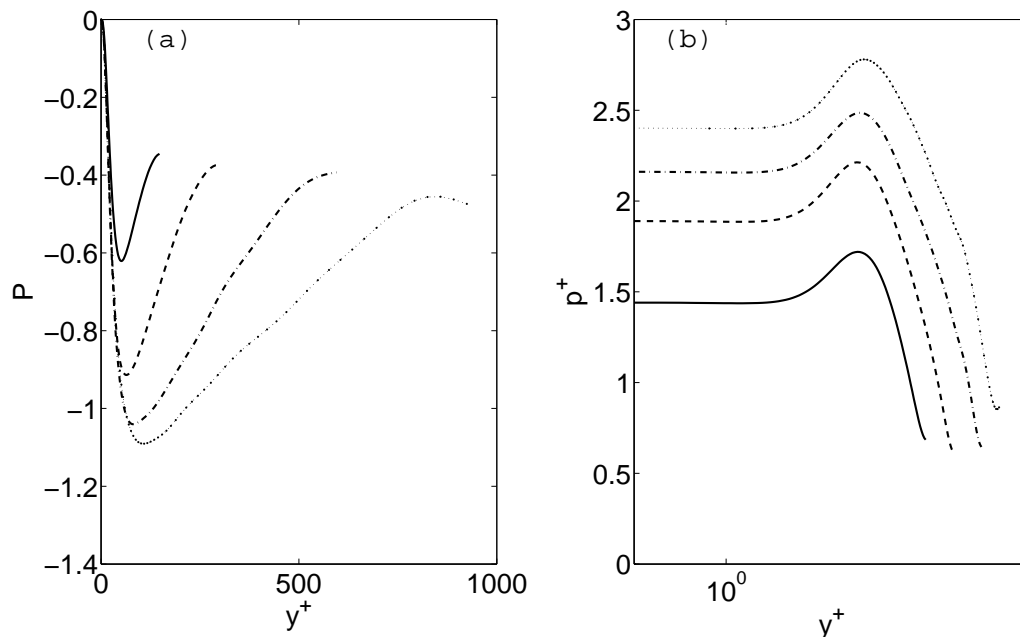


Figure 4: Mean pressure and root mean square of pressure fluctuation. Lines as in Table 1. (a) Mean pressure; (b) r.m.s.,  $p^+$ .

which are a function of the skin friction. This result shows, on the other hand, that these structures are linked, in same way, with the skin friction at the wall. Or, in other words, that these structures control the friction at the wall. Furthermore, based on the strong similarity that exist between velocity and temperature in the near-wall region, it is also expected that these structures have importance on the heat transfer at the wall (Pasinato, 2007).

Figures 4-a and 4-b show the mean pressure and the r.m.s. of the pressure fluctuation. These figures show that pressure does not scale with the inner variables; it is a function of the Reynolds number. The value of  $p^+$  increases for the different Reynolds numbers while the location of its maximum scales with the inner scales. In contrast, the mean pressure collapse at the wall for the different Reynolds numbers, but also it is a function of the Reynolds number far from the wall. In short, no one of these plots for the different Reynolds numbers collapse when nondimensionalized with the wall parameters, they all show a clear dependence on the Reynolds number.

In Table 2 the r.m.s. of some turbulent quantities at the wall are presented. In the present DNS the value of  $\epsilon$  at the wall for  $Re_\tau = 149$  is 0.155, while from a DNS for a similar flow but at  $Re_\tau = 180$  performed by Kim et al. (1987) was 0.166, which shows a reasonable agreement with the numeric value of the present study. In this table  $\epsilon$  is the total of the turbulent kinetic energy dissipation, homogeneous plus non-homogeneous; on the other hand, it was verified -no data shown- for the four Reynolds numbers that the non-homogeneous part of the turbulence dissipation of the velocity field is about 2% in the whole domain, as it was previously published by Bradshaw and Perot (1993)).

Any turbulent quantity in Table 2 shows some kind of universality based on the usual inner wall scales; all of them depend of the Reynolds number. Antonia and Kim (1994) used the Kolmogorov's inner length and velocity scales,  $\eta = (\nu^3/\epsilon_w)^{1/4}$  and  $v = (\nu\epsilon_w)^{1/4}$ , respectively, where  $\epsilon_w$  is the dissipation at the wall, and found that in the near-wall region most of the turbulence quantities scale better on Kolmogorov's scales, although not perfect, than on the

usual wall scales  $u_\tau$  and  $\nu/u_\tau$ .

In Figure 2-a and 2-d the r.m.s. of  $u$  and  $\theta$  were shown, respectively. These figures show that the values of both fluctuations do not scale with the inner variables, but the locations of the maximal for both fluctuations agree for the different Reynolds numbers. The correlation or decorrelation, similarity or dissimilarity, between both fluctuations can be measured in different ways. It can be used the second moment of both fluctuations  $\langle u\theta \rangle$  normalized by their r.m.s. as  $\rho_{u\theta} = \langle u\theta \rangle / (u^+ \theta^+)$ . But also the variance of the difference between these fluctuations, normalized by the product of the r.m.s., can be used as a measure of the similarity.

In other words, using a new variable  $\hat{\phi} = (\hat{u} - \hat{\theta})$  that, as all turbulent variables, is decomposed in a fluctuation plus a mean value,  $\hat{\phi} = \Phi + \phi$ , for  $Pr = 1$ , the fluctuation of this variable is  $\phi = (u - \theta)$  and its variance is  $\langle \phi\phi \rangle = \langle uu \rangle + \langle \theta\theta \rangle - 2\langle u\theta \rangle$ , which can be normalized by  $u^+$  and  $\theta^+$  as a measure of the dissimilarity (Pasinato, 2013, 2012). In Figure 5-a the plot of  $\phi^{+2}/(u^+ \theta^+)$  is shown. This figure shows that for the four Reynolds numbers the variance of the difference normalized presents a minimum approximately at  $y \simeq 10$  and then it increases toward the central region.

It is interesting to see what are the source terms of this variance. The conservation law of  $\langle \phi\phi \rangle$  is

$$\frac{\partial}{\partial t} \langle \phi\phi \rangle = \frac{1}{R_\tau} \frac{d^2}{dy^2} \langle \phi\phi \rangle - \frac{d}{dy} \langle \phi\phi v \rangle - 2 \langle \phi v \rangle \frac{d\Phi}{dy} - 2 \langle \phi \frac{\partial p}{\partial x} \rangle - \frac{2}{R_\tau} \langle \frac{\partial \phi}{\partial x_j} \frac{\partial \phi}{\partial x_j} \rangle \quad (1)$$

where equation (1) has been simplified for developed conditions; the term on the left (1) is zero, while the first term on the right is the molecular diffusion, the second is the turbulent transport, the third and fourth are production terms, and the last term is the dissipation of the variance of the difference between the fluctuations.

The interest here are the production terms in equation (1); the terms which are the responsible of the production of the differences between the fluctuations of longitudinal velocity and temperature. One of these terms is the third term on the right  $-2 \langle \phi v \rangle d\Phi/dy = -2(\langle uv \rangle - \langle \theta v \rangle)(dU/dy - d\Theta/dy)$ , which is the product of the difference between the wall-normal gradients of the mean fields by the difference between the wall-normal fluxes. For developed conditions this term is almost zero, and it is clearly a minor term in comparison with the other production term, the fourth term on the right of this equation,  $-2 \langle \phi \partial p / \partial x \rangle = -2(\langle u \partial p / \partial x \rangle - \langle \theta \partial p / \partial x \rangle)$ , which is a 'difference  $u - \phi$  pressure-gradient interaction' term. This term is a measure of how both turbulent fields,  $u$  and  $\theta$ , correlate with the instantaneous axial pressure gradient, and is also the only important generator of differences between  $u$  and  $\theta$  (from the conservation laws of  $\langle uu \rangle$  and  $\langle \theta\theta \rangle$ , not written here, it can be seen that the only difference between both equations is the *velocity-pressure gradient* interaction,  $-\langle u \partial p / \partial x \rangle$ , which redistributes energy among the velocity components). This term is always positive, representing a source of  $\langle \phi\phi \rangle$ , showing that the differences between  $u$  and  $\theta$  is due to a better correlation of the instantaneous axial pressure gradient with the scalar transported by the fluid than with the axial velocity.

Figure 5-b shows the distribution of the production term responsible of this variance  $\langle \phi \partial p / \partial x \rangle^+ = \langle (u - \theta) \partial p / \partial x \rangle^+$ . This figure shows that  $\langle (u - \theta) \partial p / \partial x \rangle^+$  almost scale with the inner parameters for the three higher Reynolds numbers, showing a low-Reynolds number effect only for case  $Re150$ . Data not shown here reveal that  $\langle \theta \partial p / \partial x \rangle^+$  is almost twice the value of  $\langle u \partial p / \partial x \rangle^+$  in the whole domain, increasing in the central region.

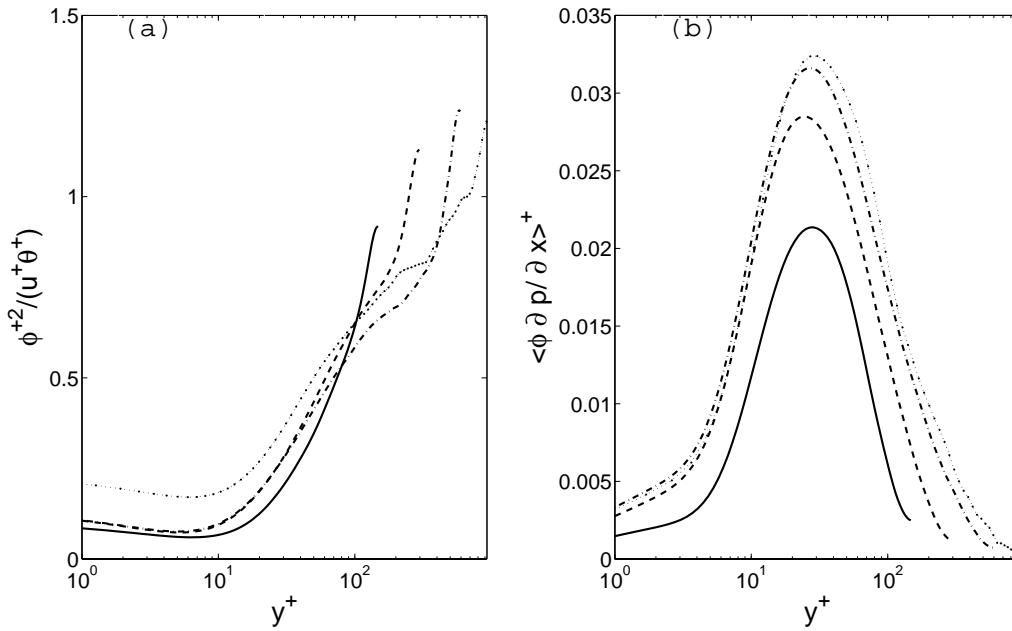


Figure 5: Normalized variance of the difference between the longitudinal velocity and temperature fluctuations, and correlation of instantaneous axial pressure gradient with the difference of the longitudinal velocity and temperature fluctuation. Lines as in Table 1. (a)  $\phi^{+2}/(u^+\theta^+) = (u - \theta)^2/(u^+\theta^+)$ ; (b)  $\langle \phi \partial p / \partial x \rangle^+$ .

Another result that deserve be commented is the dependence from the Reynolds number, of the similarity relationship between the r.m.s. of the fluctuations and the mean wall-normal gradient, for longitudinal velocity and temperature in the wall layer (Pasinato, 2013, 2012). This similarity is a consequence of the phenomenology of the momentum and heat transfer in the wall layer; e.g. almost 80% of  $u$  in the wall layer is associated with turbulent events for which  $\langle uv \rangle < 0$ , and the same is true for  $\theta$  which are associated with events for which  $\langle \theta v \rangle < 0$ . This relation is

$$\frac{(\partial U / \partial y)^+}{u^+} \simeq \frac{(\partial \Theta / \partial y)^+}{\theta^+} \quad (2)$$

where  $\theta^+$  and  $u^+$  are the r.m.s. of the fluctuations of temperature and longitudinal velocity and  $(\partial \Theta / \partial y)^+$  and  $(\partial U / \partial y)^+$  are the wall-normal mean gradient of the temperature and longitudinal velocity, respectively.

Figure 6-a and 6-b show these relationship for  $Pr = 1$  for the four  $Re_\tau$ . Since the wall-normal gradients scale with the inner variables, but not the r.m.s. of the fluctuations, these plots do not collapse in a unique plot. However it is clear that for a specific Reynolds numbers these plots are similar in the wall layer and in a major part of the central region.

#### 4 CONCLUSIONS

In this study the results of direct numerical simulations at four Reynolds numbers up to 930, for a channel flow with heat transfer is presented. The statistics of the turbulent quantities of the numerical simulations present a good agreement with similar results from the literature. Beside the mean values of the longitudinal velocity and temperature, all other turbulent quantities have a clear Reynolds number dependency (as it is already known), when scaled with the inner scales.

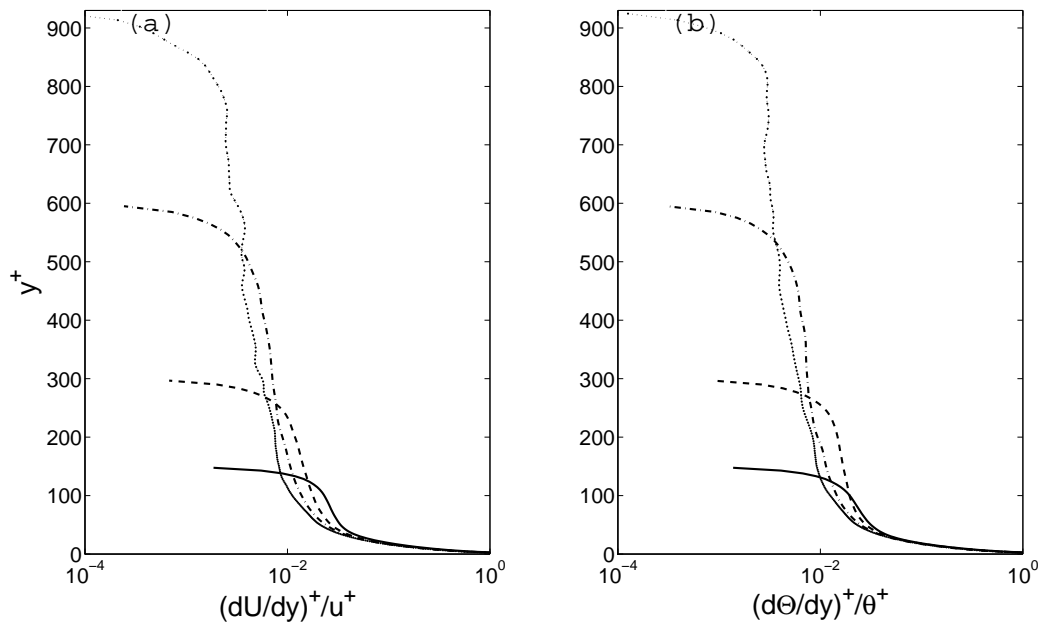


Figure 6: (a)  $(dU/dy)^+/u^+$ ; (b)  $(d\Theta/dy)^+/\theta^+$ . Lines as in Table 1.

As regarding the similarity between the r.m.s. of the fluctuations and the wall-normal gradient (for the longitudinal velocity and the temperature), the results for higher Reynolds numbers give a more solid foundation to this similarity for the wall layer.

### Acknowledgments

The numerical simulations reported here were made possible by a generous computer time provided by the Centro de Computos de Alto Desempeño, Universidad Nacional de Córdoba, at the cluster Mendieta. This support is gratefully acknowledged.

### REFERENCES

- Antonia, R. A. and J. Kim. Low-Reynolds-numbers effects on near-wall turbulence. *J. Fluid Mech.*, **276**, pp. 61-80, 1994.
- Barenblatt, G.I. Scaling law for fully developed turbulent shear flow. Part 1. Basic hypotheses and analysis. *J. Fluid Mech.*, **248**, pp. 513-20, 1993.
- Bradshaw, P. and B. Perot A note on turbulent energy dissipation in the viscous wall region, *Physics of Fluid A*, **512**, pp. 3305-3306, 1993.
- Dean, R.B. Reynolds Number Dependence of Skin Friction and Other Bulk Flow Variables in Two-Dimensional Rectangular Duct Flow. *J. Fluid Eng.*, **200**, pp. 215-23, 1978.
- Hites, M. H. Scaling of high-Reynolds number turbulent boundary layers in the National Diagnostic Facility. Ph. D. Thesis, Illinois Inst. of Technology, 1997.
- Hoyas, S. and Jimenez, J. Reynolds number effect on the Reynolds-stress budgets in turbulent channel. *Physics of Fluids.*, **20**-101511, 2008.
- Jimenez, J. and Sergio Hoyas. Turbulent fluctuations above the buffer layer of the wall-bounded flows. *J. Fluid Mech.*, **611**, pp. 215-236, 2008.
- Jiménez, J. The largest structures in turbulent wall flows. Annual Research Briefs, Center for Turbulence Research, NASA Ames/Stanford Univ., pp. 943-945, 1998.
- Kader, B.A. Temperature and Concentration Profiles in Fully Turbulent Boundary Layers. *Int.*

- J. Heat Mass Transfer*, **24**(9), 1541-1544, 1981.
- Kim, J., P. Moin and R. Moser. Turbulence statistics in fully developed channel flow at low Reynolds number. *J. Fluid Mech.*, **177**, pp. 133-166, 1987.
- Kim, J. and P. Moin. Transport of Passive Scalar in a Turbulent Channel Flow. In *Turbulent Shear Flow*, 6:86-96, 1989.
- Kim, C.K. and R.J. Adrian. Very large-scale motion in the outer layer. *Physics of Fluids*, **11**, pp. 417, 1999.
- Kozuka, M., Seki, Y. and Kawamura, H. Direct numerical simulation of turbulent heat transfer with a high spatial resolution, Proc. of the 7rd International Symposium on Engineering Turbulence Modeling and Measurements -ETMM7, vol. 1, pp. 163-168, 2008.
- Marusic, I., B.J. McKeon, P.A. Mokevitz, H.M. Nagib, A.J. Smits, and K.R. Sreenivasan. Wall-bounded turbulent flows at high Reynolds numbers: Recent advances and key issues *Physics of Fluids*, **22**-065103, 2010.
- Millikan, C.M. A Critical Discussion of Turbulent Flows in Channels and Circular Tubes, in Proceeding of the 5th. International Congress of Applied Mechanics, Wiley, New York, pp. 386-392, 1993.
- Moser, R.D., J. Kim and N.N. Mansur. Direct numerical simulation of turbulent channel flow up to  $Re_\tau = 590$ . *Physics of Fluids*, **11**-4, pp. 943-945, 1999.
- Pasinato, H.D. Velocity and Temperature Natural Dissimilarity in a Turbulent Channel Flow, *Mecánica Computacional*, **XXVI**; S.A. Elaskar, E.A. Pilotta, and G.A. Torres (Eds), pp. 3644-3663, 2007 (<http://www.cimec.org.ar/ojs/index.php/mc>).
- Pasinato, H.D. Velocity and Temperature Dissimilarity in Fully Developed Turbulent Channel and Plane Couette Flows, *Int. J. Heat and Fluid Flow*, 32:11-25, 2011.
- Pasinato, H.D. Dissimilarity of Turbulent Fluxes of Momentum and Heat in Perturbed Turbulent Flows, submitted to ASME *J. Heat Transfer*, 2013.
- Pasinato, H.D. 2012 Wall-layer turbulent heat transfer modeling for perturbed flows, in *Mec. Computacional*, **XXXI**, Eds. Cardona, A., Khoan, P., Quinteros, R., M. Storti, pp. 2059-2073. <http://www.amcaonline.org.ar>.
- Tennekes H. and J. L. Lumley, *A First Course in Turbulence*, MIT Press, Cambridge, 1990.
- Townsend, A.. *The Structure of Turbulent Shear Flow*, 2nd. edn. Cambridge University Press, 1976.
- Wei T. and W.W. Willmarth. Reynolds-number effects on the structure of a turbulent channel flow. *J. Fluid Mech.*, **26**, pp. 57-95, 1989.
- Wosniki M., L. Castillo, and W.K. George. A theory for turbulent pipe and channel flows. *J. Fluid Mech.*, **421**, pp. 115-145, 2000.